Exposure at the Cell Surface Is Required for Gas3/PMP22 To Regulate Both Cell Death and Cell Spreading: Implication for the Charcot–Marie–Tooth Type 1A and Dejerine–Sottas Diseases

Claudio Brancolini,[*†§] **Paolo Edomi,**[†‡] **Stefania Marzinotto,**[†] **and Claudio Schneider**[†]

[*]Dipartimento di Scienze e Tecnologie Biomediche, Sezione di Biologia, Universita' di Udine, 33100 Udine, Italy; [†]Laboratorio Nazionale Consorzio Interuniversitario Biotecnologie AREA Science Park, Padriciano 99 34142 Trieste, Italy; [‡]Dipartimento di Biologia Universita' di Trieste, 34100 Trieste, Italy

Gas3/PMP22 is a tetraspan membrane protein highly expressed in myelinating Schwann cells. Point mutations in the *gas3/PMP22* gene account for the dominant inherited peripheral neuropathies Charcot–Marie–Tooth type 1A disease (CMT1A) and Dejerine–Sottas syndrome (DSS). Gas3/PMP22 can regulate apoptosis and cell spreading in cultured cells. *Gas3/PMP22* point mutations, which are responsible for these diseases, are defective in this respect. In this report, we demonstrate that Gas3/PMP22-WT is exposed at the cell surface, while its point-mutated derivatives are intracellularly retained, colocalizing mainly with the endoplasmic reticulum (ER). The putative retrieval motif present in the carboxyl terminus of Gas3/PMP22 is not sufficient for the intracellular sequestration of its point-mutated forms. On the contrary, the introduction of a retrieval signal at the carboxyl terminus of Gas3/PMP22-WT leads to its intracellular accumulation, which is accompanied by a failure to trigger cell death as well as by changes in cell spreading. In addition, by substituting the Asn at position 41 required for N-glycosylation, we provide evidence that N-glycosylation is required for the full effect on cell spreading, but it is not necessary for triggering cell death. In conclusion, we suggest that the DSS and the CMT1A neuropathies derived from point mutations of *Gas3/PMP22* might arise, at the molecular level, from a reduced exposure of Gas3/PMP22 at the cell surface, which is required to exert its biological functions.

INTRODUCTION

Gas3/PMP22, a 22-kDa glycoprotein, is a member of an extended family of tetraspan membrane proteins that seems to be well conserved among different species (Agostoni *et al.*, 1999; Wulf *et al.*, 1999). Studies in cultured cells have demonstrated that Gas3/PMP22 can regulate cell death and cell spreading both in fibroblasts and Schwann cells (Fabbretti *et al.*, 1995; Brancolini *et al.*, 1997; Zoidl *et al.*, 1997; Baudet *et al.*, 1998). The effect on cell spreading was dependent on the small GTPase Rho since the coexpression of activated Rho or

the treatment of the cells with bacterial toxins regulating Rho GTP status can modulate the Gas3/PMP22-dependent effect on cell spreading (Brancolini *et al.*, 1999).

Although Gas3/PMP22 expression has been detected in different tissues, both in adult mice and during development of mice (Baechner *et al.*, 1995), its expression is highly induced in myelinating Schwann cells. Gas3/PMP22 accounts for 2–5% of the total myelin proteins largely confined to compact myelin (Spreyer *et al.*, 1991; Welcher *et al.*, 1991; Snipes *et al.*, 1992).

Genetic studies demonstrating that *gas3/PMP22* is responsible for a set of inherited peripheral neuropathies in mice and humans (Patel and Lupski, 1994; Adlkofer *et al.*, 1995; Suter and Snipes, 1995; Huxley *et al.*, 1996; Magyar *et al.*, 1996; Sereda *et al.*, 1996) strongly argue for an important function of Gas3/PMP22 in myelin membrane formation/maintenance.

The most common form of Charcot–Marie–Tooth type 1 (CMT1) disease, CMT1A, a peripheral neuropathy that re-

§ Corresponding author. E-mail address: cbrancolini@makek.dstb.uniud.it.

Abbreviations used: CMT1A, Charcot-Marie-Tooth type 1A; DMEM, Dulbecco's minimum essential medium; DSS, Dejerine–Sottas syndrome; Endo-H, endoglycosidase H; FCS, fetal calf serum; hPLAP, human placental alkaline phosphatase; PBS, phosphate-buffered saline; PCR, polymerase chain reaction; SDS, sodium dodecyl sulfate.

sults in progressive atrophy of distal muscles and impaired sensation of the limbs, is characterized by genomic duplication on 17p11.2-p12 containing the *gas3/PMP22* locus (Lupski *et al.*, 1991; Matsunami *et al.*, 1992; Patel *et al.*, 1992; Timmerman *et al.*, 1992; Valentijn *et al.*, 1992b).

In addition, more than 30 point mutations in the *gas3/PMP22* gene have been found in nonduplication CMT1A families and in the related severe congenital hypertrophic neuropathy Dejerine–Sottas syndrome (DSS) (Valentijn *et al.*, 1992a; Roa *et al.*, 1993a, b; Kovach *et al.*, 1999; Nelis *et al.*, 1999). More recently, *gas3/PMP22* point mutations responsible for both CMT1A and DSS also have been associated with deafness (Ionasescu *et al.*, 1996; Kovach *et al.*, 1999).

A large portion of the point mutations that have been identified are located in the transmembrane domains. Several studies indicate that these point mutations act by a gain-of-function mechanism that usually causes more severe disease than is the case with *gas3/PMP22* duplication (Hanemann and Muller, 1998). More recently, it has been reported that some point-mutated forms of gas3/PMP22 accumulate intracellularly and are impaired in transport to the cell surface (Naef *et al.*, 1997; D'Urso *et al.*, 1998; Naef and Suter, 1999; Tobler *et al.*, 1999).

We have recently demonstrated that *gas3/PMP22* point mutations responsible for CMT1A and DSS were also defective in inducing cell death and changes in cell spreading, thus indicating a direct link between the disease and the observed phenotypes (Brancolini *et al.*, 1999).

In this report, we have investigated the molecular mechanisms responsible for this observation, demonstrating by different approaches that Gas3/PMP22-WT, but not the point-mutated derivatives L16P, S79C, and G150D, is exposed at the cell surface. The putative retention/retrieval motif present in the carboxyl terminus of Gas3/PMP22 is not sufficient for the intracellular sequestration of its point-mutated forms. The introduction of a retrieval signal at the carboxyl terminus of Gas3/PMP22-WT leads to its intracellular accumulation. This intracellularly retained Gas3/PMP22 was unable to trigger cell death as well as changes in cell spreading.

In addition, by substituting the Asn at position 41, which is required for N-glycosylation, we provide evidence that N-glycosylation is not necessary for cell death but is indispensable for a full effect on cell spreading.

MATERIALS AND METHODS

Culture Conditions and Microinjection

NIH3T3 and COS-7 cells were grown in Dulbecco's minimum essential medium (DMEM) supplemented with 10% fetal calf serum (FCS), penicillin (100 U/ml), and streptomycin (100 μg/ml).

For microinjection assays, cells were grown on coverslips in 35-mm Petri dishes containing 8×10^4 cells per dish. After a 24-h incubation period at 37°C in a 5% CO_2 atmosphere, cells were microinjected with the appropriate expression plasmids.

Nuclear microinjection was performed using the Automated Injection System (Zeiss, Jena, Germany) as previously described (Fabbretti *et al.*, 1995). Nuclei were injected with the different expression vectors for 0.5 s at a constant pressure of 150 hPA. Statistical significance was determined for all data by using one-way analysis of variance (F-test).

For transfection, COS-7 cells were washed twice with DMEM, then DMEM containing 0.5 mg/ml DEAE-dextran and 10 μg of DNA was added. After incubation at 37°C for 30 min, DMEM containing 10% FCS and chloroquine (100 μM) was added and incubation was prolonged for 4 h. Cells then were washed twice with DMEM and were grown for 2 days in DMEM containing 10% FCS.

Immunofluorescence Microscopy

For indirect immunofluorescence microscopy, microinjected NIH3T3 cells were fixed with 3% paraformaldehyde in phosphate-buffered saline (PBS) for 20 min at room temperature. Fixed cells were washed with PBS/0.1 M glycine, pH 7.5, and then were permeabilized with 0.1% Triton-X100 in PBS for 5 min. The coverslips were treated with different first antibodies, such as anti-FLAG (Sigma, St. Louis, MO), anti-vesicular stomatitis virus (VSV) (Sigma), and anti-human placental alkaline phosphatase (hPLAP), or with biotinylated concanavalin A (Boehringer, Mannheim, Germany) diluted in PBS, and with 3% BSA for 1 h in a moist chamber at 37°C. The coverslips then were washed with PBS three times, followed by incubation with the relative secondary antibodies fluorescein isothiocyanate-conjugated antimouse (Sigma), tetramethyl-rhodamine isothiocyanate (TRITC)-conjugated antimouse (Southern Biotechnology, Birmingham, AL), TRITC-conjugated antirabbit (Dako, Carpinteria, CA), fluorescein isothiocyanate-conjugated antirabbit (Sigma), or TRITC-conjugated streptavidin (Jackson ImmunoResearch Laboratories, West Grove, PA) for 1 h at 37°C. Cells were examined by epifluorescence with a Zeiss Axiovert 35 microscope or a Zeiss laser scan microscope (LSM 410) equipped with a 488 λ argon laser and a 543 λ helium neon laser.

In Vivo Biotinylation

After transfection with the appropriate plasmid, COS-7 cells were washed twice with PBS and then were incubated twice for 30 min with freshly prepared biotin-3-sulfo-N-hydroxysuccinimide (Pierce Chemical, Rockford, IL) 0.2 mg/ml in PBS. After quenching with 50 mM Tris-HCl, pH 7.5, cells were resuspended in 1 ml of lysis buffer (50 mM Tris-HCl, pH 7.5, 150 mM NaCl, and 1% Triton X-100), containing 1 mM phenylmethylsulfonyl fluoride and 10 mg/ml each of aprotinin, leupeptin, antipain, and pepstatin. After centrifugation, 50 μl of streptavidin–agarose (30% wt/wl) suspension was added, and the incubation was continued for 1 h by rocking at room temperature. The streptavidin–agarose suspension was recovered by centrifugation and was washed several times in lysis buffer. Complexes were released by boiling for 5 min in sodium dodecyl sulfate (SDS) sample buffer, separated by SDS-polyacrylamide gel electrophoresis or Tris/Tricine buffer, and Western blots were performed.

Proteins in the supernatant were precipitated by the addition of acetone (80% final concentration), incubation on ice for 20 min, and centrifugation.

Enzymatic Treatment Immunoblotting

PNGase-F treatment of cellular lysates and immunoblotting analysis were performed as described (Fabbretti *et al.*, 1995). For endoglycosidase H (Endo-H) (Boehringer) treatment, the cellular lysates were prepared in 0.5% SDS and 1% β-mercaptoethanol, were denatured by boiling for 10 min, and then 50 mM sodium acetate, pH 5.5, and 1% NP40 was added. After the addition of 1 milliunit of Endo-H, samples were incubated for 3 h at 37°C. For sialidase treatment, the lysates were denatured as above and then incubated in 50 mM sodium phosphate, pH 6, and 1% NP40 in the presence of 10 milliunits of neuraminidase (sialidase, Boehringer) for 3 h at 37°C.

Plasmid Construction

For expression in eukaryotic cells, human *gas3/PMP22* (Edomi *et al.*, 1993) and point mutant forms L16P, S79C, and G150D (Fabbretti *et*

al., 1995) were amplified by polymerase chain reaction (PCR) and were subcloned in frame with a C-terminal VSV tag in pGDSV7-VSV vector. The sense primer ol5′ (5′-GAGTGAATTCAACTC-CGCTGAGCAGAACTT-3′) containing an *Eco*RI site and a reverse primer ol3′tag (5′- CGCAAGCTTTTCGCGTTTCCGCAAGATCA -3′) containing an *Hin*dIII site were used.

Mutant forms of *hgas3/PMP22* with potential endoplasmic reticulum localization dibasic motifs, di-lysine (KK) or di-arginine (RR) (Teasdale and Jackson, 1996) were constructed by PCR using human *gas3/PMP22* (Edomi *et al.*, 1993) as template. The amplified fragments were subcloned in the pGDSV7-VSV vector. For RR-*hgas3/PMP22*-VSV construction, the sense primer ol5′RR (5′- GGGAAT-TCCGCCAGAATGTCCCGCCGCTCCCTCCTCCTGTTGCTGAGT -AT -3′), containing an *Eco*RI site, a Kozak sequence, and a sequence coding for the Ser-Arg-Arg-Ser motif, and the reverse primer ol3′tag were used. For *hgas3/PMP22*-KK-VSV construction, the sense primer ol5′ and the reverse primer ol3′KK (5′- TTTCCGCGGTCAGGAA-GACTTCTTCTTTCCAAGTCGGTTCATCTC -3′), containing a sequence coding for Lys-Lys-Ser-Ser motif, a stop signal, and a *Sac*II site, were used.

hgas3/PMP22 and the point mutant L16P, in which the potential endoplasmic reticulum retention motif Arg-Lys-Arg (Zerangue *et al.*, 1999) was substituted with three Ala (the aa from 157 to 159), were constructed by PCR. The sense primer ol5′ and the reverse primer ol3′-3ala (5′- CGAAAGCTTTTCGGCTGCCGCCAAGAT-CACATAGATGAC -3′) were used, and the amplified fragments were subcloned in pGDSV7-VSV vector.

A site-directed mutagenesis method by overlap extension through PCR (Fabbretti *et al.*, 1995) was used to produce the glycosylation mutant form of hGas3. As external primers the ol5′ and ol3′ tag oligonucleotides were used. The pair of complementary inverse oligonucleotides used to insert the mutation Asn → Gln at position 41 were the following: olnoG (5′-CTCTGGCAGCAATGTAGCACC-3′) and olnoG′ (5′-GGTGCTACAGTTCTGCCAGAG-3′).

Gas3/PMP22 containing paired VSV tags at the carboxyl terminus was created by inserting a linker encoding the VSV epitope at the *Hin*dIII site of pGDSV7S-*hgas3/PMP22-VSV*: (5′-AGCTTTC-CCCTTCCCCTTATACAGACATAGAGATGAACCGACTTGGAA-3′).

All constructs generated were sequenced using an automated (ALF) system to check for the respective mutations introduced and for the fidelity of the inserted PCR fragments.

RESULTS

Analysis of the Electrophoretic Mobility of the Epitope-Tagged Gas3/PMP22 and Its Point-Mutated Derivatives

We have recently demonstrated that Gas3/PMP22 can regulate cell death and cell spreading when overexpressed in cultured cells and that the latter response is dependent on the small GTPase Rho. Gas3/PMP22 point-mutated derivatives responsible for CMT1A and the DSS are defective in these functions (Brancolini *et al.*, 1999). To gain more insight into the impaired ability of the Gas3/PMP22 point mutants to regulate cell spreading and cell death, we epitope-tagged Gas3/PMP22-WT and its point-mutated derivatives responsible for CMT1A, Gas3/PMP22-L16P, Gas3/PMP22-S79C, as well as Gas3/PMP22-G150D, which is responsible for DSS. Both the VSV and FLAG tags were introduced at the carboxyl terminus of Gas3/PMP22, as described in Materials and Methods. Western blot analysis was performed on lysates from transfected COS-7 cells to compare the electrophoretic profile of the epitope-tagged proteins with the untagged ones.

As previously described (Fabbretti *et al.*, 1995), an antibody specific for hGas3/PMP22 recognizing the first extracellular loop was only able to recognize hGas3/PMP22 expressed in cultured cells after treatment with N-glycosidase F (*PNGase-F*) (Figure 1a). This was possibly due to steric hindrance caused by the sugar chain. Recognition of the hGAS3/PMP22 glycosylated form in phrenic nerves by the same anti-hGas3/PMP22 antibody (Figure 1a) might depend on Schwann cell–specific processing of the mature sugar chain.

As shown in Figure 1a, the anti-Gas3/PMP22 antibody recognizes a major band migrating around 18 kDa after *PNGase-F* treatment both in Gas3/PMP22-WT and in Gas3/PMP22-L16P-transfected COS-7 cell lysates. Moreover, a faint band migrating at around 18 kDa also was detected in the lysates of untreated Gas3/PMP22-WT-transfected cells. This band shows electrophoretic mobility similar to the one recognized in *PNGase-F*-treated phrenic nerve lysates and, therefore, might represent a form of Gas3/PMP22 lacking N-linked sugar chains. The lower migrating bands detected in the extracts of the human phrenic nerves probably represent proteolytic fragments generated by postmortem proteolysis.

COS-7 cells then were transfected with *Gas3/PMP22-WT* and Gas3/PMP22-L16P, VSV and FLAG epitope-tagged forms, and Western blot analysis was performed using the respective antibodies.
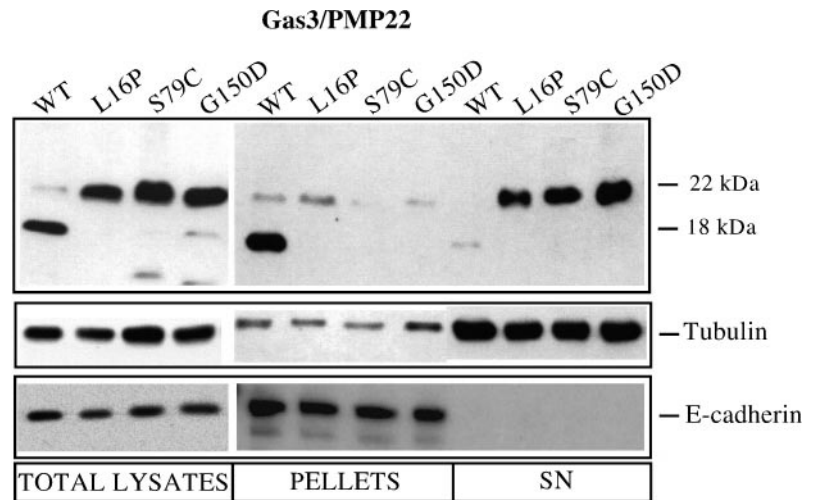
Both Gas3/PMP22-WT-VSV and Gas3/PMP22-WT-FLAG were detected as bands migrating at ~18 kDa, the intensity of which dramatically increased after *PNGase-F* treatment. These bands show the same electrophoretic mobility as the band detected by the anti-hGas3/PMP22 antibody in both phrenic nerves and in transfected cells after *PNGase-F* treatment. Both the anti-VSV and the anti-FLAG antibodies were unable to detect the mature form of Gas3/PMP22-WT that should migrate at 22 kDa (Manfioletti *et al.*, 1990), thus indicating that the N-linked oligosaccharide chain present in the first extracellular loop probably masks the tag epitopes, even though they are located at the carboxyl terminus of the protein. Moreover, in the case of both the Gas3/PMP22-VSV and the Gas3/PMP22-FLAG, a band migrating with the same electrophoretic mobility of the *PNGase-F*-treated Gas3/PMP22 was detected in untreated cell lysates. This band could represent a form of Gas3/PMP22 that lacks the N-linked oligosaccharide, as previously observed in the case of the anti-hGas3/PMP22 antibody.

A different electrophoretic pattern was observed in the case of epiptope-tagged Gas3/PMP22-L16P. Here, a band migrating at ~22 kDa was observed, the electrophoretic mobility of which was reduced to 18 kDa by *PNGase-F* treatment.

We next analyzed whether other epitope-tagged point-mutated derivatives of Gas3/PMP22 exhibited a different electrophoretic mobility with respect to the WT form.

As shown in Figure 1b, the point-mutated Gas3/PMP22-G150D and Gas3/PMP22-S79C also were detected in Western blots as 22-kDa bands, thus exhibiting an electrophoretic mobility similar to the point-mutated L16P. *PNGase-F* treatment of the different point-mutated Gas3/PMP22 derivatives produced an 18-kDa band showing similar electrophoretic mobility to the WT form, thus suggesting that the 4-kDa difference in electrophoretic mobility was due to a

Figure 1. Expression of the epitope-tagged Gas3/PMP22 and its point-mutated derivatives. (a) Characterization of the VSV and FLAG epitope-tagged Gas3/PMP22-WT and Gas3/PMP22-L16P. Immunodetection of Gas3/PMP22 in the phrenic nerve and in COS-7 cells transfected with Gas3/PMP22-WT and Gas3/PMP22-L16. COS-7 cells were transfected as described in Materials and Methods with the indicated plasmids and immunodetection performed with the indicated antibodies. (b) Immunodetection of VSV epitope-tagged Gas3/PMP22-WT and its point-mutated derivatives on transfected COS-7 cells. (c) Immunodetection of Gas3/PMP22 containing a paired VSV at its carboxyl terminus. Tissue and cellular extracts were treated with or without PNGase-F, as described in Materials and Methods.

N-linked oligosaccharide. Therefore, the sugar chain present in the mutated Gas3/PMP22 does not impair the detection of the epitope tag.

The inability of the antiepitope antibodies to detect the mature form of Gas3/PMP22-WT prompted us to investigate whether indeed the carbohydrate structure might mask the epitope. We postulated that by expanding the VSV sequence we could render the epitope more readily detectable by its respective antibody. Therefore, we introduced a second VSV epitope at the carboxyl terminus of Gas3/PMP22, as described in Materials and Methods. The introduction of paired VSV epitope tags did not interfere with the ability of

Gas3/PMP22

Figure 2. In vivo biotinylation of plasma membrane proteins. COS-7 cells transfected with the indicated *Gas3/PMP22-VSV* constructs were subjected to in vivo biotinylation of plasma membrane proteins as described in Materials and Methods. Immunodetection was performed using antibodies against VSV, tubulin, and E-cadherin.

Gas3/PMP22 to regulate cell death and spreading (our unpublished results). Western blot analysis was performed on lysates from transfected COS-7 cells to compare the electrophoretic profile of Gas3/PMP22 containing paired VSV (Gas3/PMP22-WT-2VSV) with Gas3/PMP22-WT-VSV.

As shown in Figure 1c, a complex electrophoretic pattern was observed in COS-7 cells transfected with *hgas3/PMP22-WT-2VSV*. Two bands migrating at ~22 and 18 kDa representing, respectively, the glycosylated and the unglycosylated forms of Gas3/PMP22 were detected. In addition, an unresolved smear ranging from 30 up to 50 kDa was observed. To gain more insight into the complex electrophoretic pattern observed in the case of Gas3/PMP22–2VSV, cellular lysates were treated with PNGase-F. The treatment of the cell lysates overexpressing Gas3/PMP22–2VSV with PNGase-F produced only the 18-kDa band, thus suggesting that the complex electrophoretic pattern was due to heterogeneity in the oligosaccharide chains (Kaushal *et al.*, 1994).

Gas3/PMP22-WT, but not Its Point-Mutated Derivatives, Is Exposed at the Cell Surface

The different results obtained in Western blotting, in terms of detection of the epitope tags when fused to the point-mutated forms of Gas3/PMP22 or to the WT, could be ascribed to different carbohydrate structures. An alteration in the carbohydrate processing could be dependent on impaired intracellular processing as a consequence of altered cellular trafficking. By immunofluorescence analysis, we have observed that the different point-mutated Gas3/PMP22 derivatives are localized in the ER, while the WT form shows a uniform distribution possibly at the cell surface (our unpublished results).

To clearly establish that Gas3/PMP22-WT, but not its point-mutated derivatives, is exposed at the cell surface, we biotinylated the cell surface of COS-7 cells transfected with the Gas3/PMP22-WT or with the point mutants L16P, S79C, and G150D.
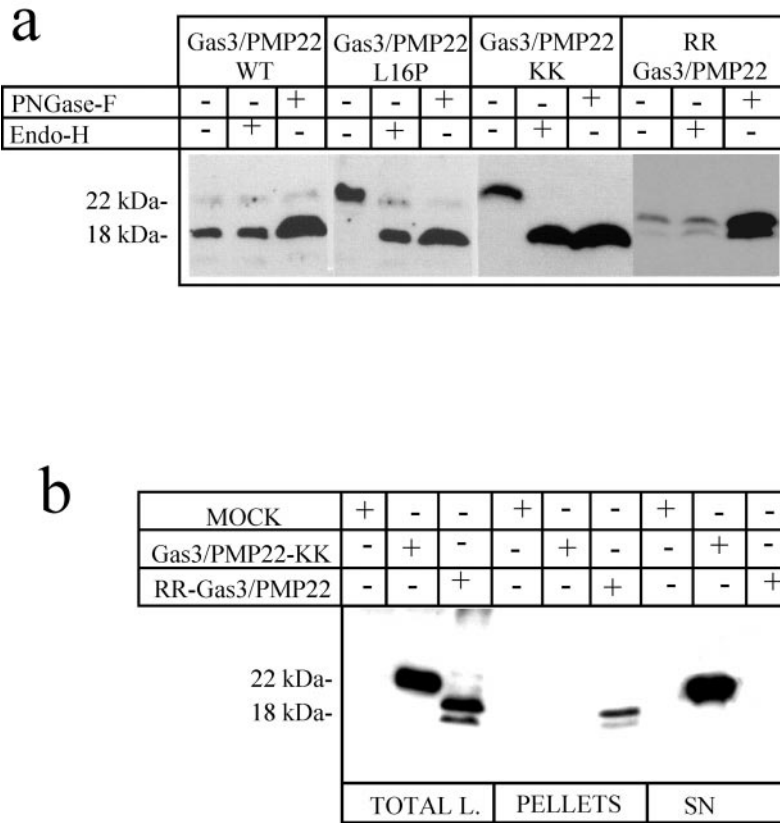
Cells were exposed to the nonpermeable biotin-3-sulfo-N-hydroxysuccinimide ester, and the biotinylated proteins then were collected by incubation with streptavidin agarose.

Western blot analysis was performed using anti-FLAG and anti-VSV antibodies to visualize Gas3/PMP22 and the different point mutants. Figure 2 shows the results obtained using anti-VSV antibody. Similar results were obtained when the FLAG detection system was used (our unpublished results). After incubation with streptavidin-agarose, Gas3/PMP22-WT was detected in the pellet fractions while the different point mutants used were present in the supernatants. This result demonstrates that only Gas3/PMP22-WT was biotinylated, thus suggesting that Gas3/PMP22 is exposed at the cell surface while its point-mutated derivatives are unable to reach the plasma membrane. It is interesting to note that the 18-kDa unglycosylated form of Gas3/PMP22-WT was biotinylated, suggesting that it is exposed at the cell surface. It is not yet clear whether this is due to a deglycosylation process or to a failure to efficiently N-glycosylate a fraction of Gas3/PMP22-WT.

Treatment of the pellet fractions with PNGase-F produced a dramatic increase in the amount of Gas3/PM22 detected by Western blot analysis, while the point-mutated forms were undetectable (data not shown), as was the case previously. This evidence indicates that the majority of Gas3/PMP22-WT exposed at the cell surface was N-glycosylated. The same lysates also were analyzed for E-cadherin as a marker for plasma membrane proteins, and for Tubulin as a marker for cytosolic proteins, to verify the quality of the biotinylation (Figure 2).

Generation of a Gas3/PMP22-WT Form That Is Intracellularly Retained

Previous experiments demonstrated that the Gas3/PMP22 point-mutated derivatives were impaired in their ability to reach the cell surface, and this correlates with a failure to trigger apoptosis and cell-shape changes when they were overexpressed in cultured cells (Brancolini *et al.*, 1999). The different point mutations used encode for an amino acid substitution in the transmembrane domains of Gas3/PMP22. It is possible that these mutations cause an altered folding of Gas3/PMP22 and that this alteration is critical for its biological function. Alternatively, it is also conceivable

a

	Gas3/PMP22 WT			Gas3/PMP22 L16P			Gas3/PMP22 KK			RR Gas3/PMP22		
PNGase-F	−	−	+	−	−	+	−	−	+	−	−	+
Endo-H	−	+	−	−	+	−	−	+	−	−	+	−

22 kDa-
18 kDa-

b

	TOTAL L.			PELLETS			SN		
MOCK	+	−	−	+	−	−	+	−	−
Gas3/PMP22-KK	−	+	−	−	+	−	−	+	−
RR-Gas3/PMP22	−	−	+	−	−	+	−	−	+

22 kDa-
18 kDa-

Figure 3. Generation of an intracellularly retained form of Gas3/PMP22. (a) Immunodetections were performed using antibodies against VSV on lysates from COS-7 cells transfected with the indicated *Gas3/PMP22-VSV* constructs. Cellular extracts were treated with or without PNGase-F and Endo-H, as indicated. (b) COS-7 cells transfected with the indicated *Gas3/PMP22-VSV* constructs were subjected to in vivo biotinylation of plasma membrane proteins, as described in Materials and Methods.

that Gas3/PMP22 must be present at the cell surface to regulate cell death and cell spreading and that the point mutations interfere merely with the intracellular trafficking.

To discriminate between these possibilities, we created a Gas3/PMP22 that is unable to reach the plasma membrane; however, we avoided the introduction of point mutations in the transmembrane domains.

The retention of membrane protein in the endoplasmic reticulum is mediated by discrete dibasic motifs: amino-terminal di-arginine (XXRR) or carboxyl-terminal di-lysine (KKXX) (Teasdale and Jackson, 1996). The RR and the KK retention signals were inserted, respectively at the amino and carboxyl terminus of Gas3/PMP22-VSV and were surrounded by serine residues to locate the dibasic residues at the positions required for ER retention (Jackson *et al.*, 1990; Schutze *et al.*, 1994).

COS-7 cells were transfected with Gas3/PMP22-WT, the point mutant L16P and with the Gas3/PMP22-WT containing the KK and the RR motifs.

To confirm further that different carbohydrate chains are present in the surface exposed or in the intracellularly retained forms of Gas3/PMP22, cell lysates were treated with Endo-H and PNGase-F (Figure 3a). Endo-H removes only high mannose-containing carbohydrates that have not been cleaved by mannosidase II, an enzyme found in the medial, trans-Golgi (Kornfeld and Kornfeld, 1985).

Incubation of the cellular lysates with PNGase-F increased the amount of detected Gas3/PMP22. Treatment of the same lysates with Endo-H did not provoke changes in the amount

of the 18-kDa band detected by Western blot analysis. Gas3/PMP22 L16P was sensitive to Endo-H treatment, thus further confirming its accumulation in an intracellular compartment before the Golgi (Figure 3a). Gas3/PMP22-KK was sensitive to Endo-H treatment, as was L16P, thus suggesting a similar intracellular localization. In the case of RR-Gas3/PMP22, only PNGase-F treatment increased the amount of detected protein, which is similarly to that of Gas3/PMP22-WT. It is interesting to note that RR-Gas3/PMP22 was detected as a doublet migrating at around 18 kDa also after PNGase-F treatment. Therefore, it is possible that the doublet represents a post-translational modification unrelated to glycosylation. We have also analyzed whether sialic acid residues could be detected in Gas3/PMP22 by treating lysates from COS-7–transfected cells with sialidase, which removes neuroaminic acids from sugar chains. Sialidase treatment was unable to modify the electrophoretic mobility of Gas3/PMP22, while β1 integrin, used as a positive control, was sensitive to sialidase activity (our unpublished results).

As a next step, we biotinylated the cell surfaces of COS-7 cells transfected with *Gas3/PMP22-KK* or with *RR-Gas3/PMP22* to clearly establish whether Gas3/PMP22-KK was intracellularly retained. Western blot analysis was performed using anti-VSV antibody to visualize the overexpressed proteins. As shown in Figure 3b, RR-Gas3/PMP22 was detected in the pellet fractions, while Gas3/PMP22-KK was present in the supernatants. This confirms that RR-
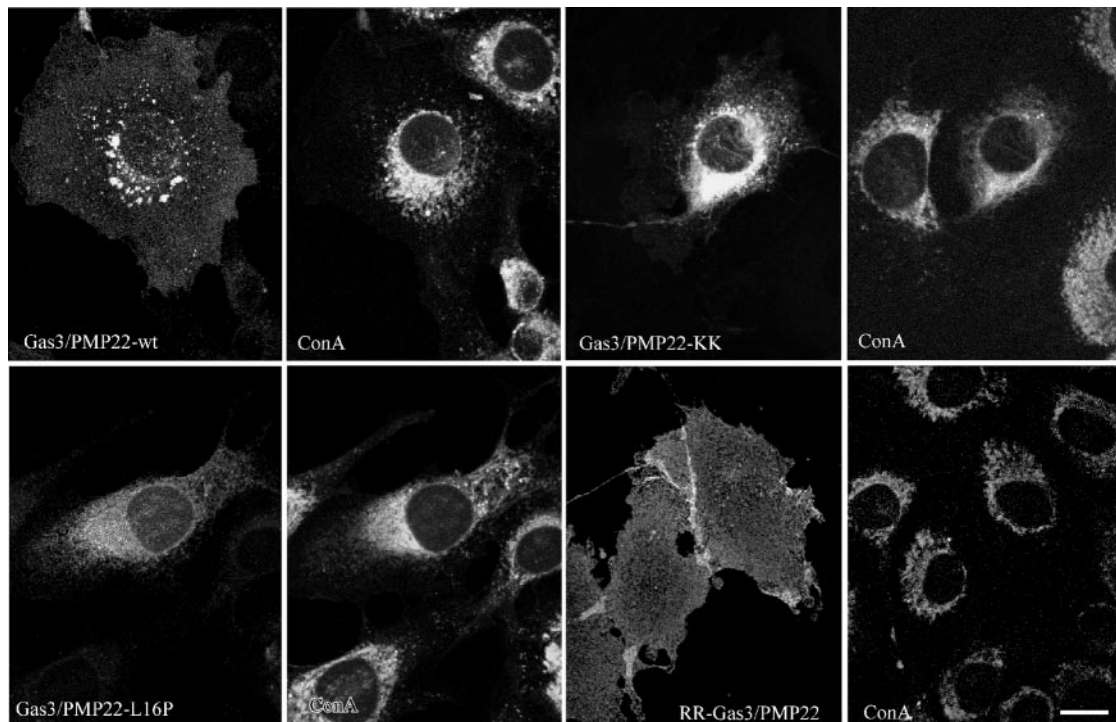
Figure 4. Subcellular localization of Gas3/PMP22-KK or RR-Gas3/PMP22 in NIH3T3 fibroblasts. Fifteen hours after microinjection, cells were fixed and double stained to visualize VSV and ER, using biotinylated concanavalin A (ConA). Bar = 15 μm.

Gas3/PMP22 was exposed at the cell surface, while Gas3/PMP22-KK was unable to reach the plasma membrane.

Finally, the different subcellular localizations of Gas3/PMP22-KK and RR-Gas3/PMP22 were analyzed by immunofluorescence. NIH3T3 cells were microinjected with expression plasmid containing *Gas3/PMP22-WT*, *Gas3/PMP22-L16P*, *Gas3/PMP22-KK*, and *RR-Gas3/PMP22*. Double-immunofluorescence analysis using biotinylated concanavalin A, a lectin that is specific for mannose residues, which are enriched in the ER compartment, and the anti-VSV antibody was performed as described in the Materials and Methods. As shown in Figure 4, Gas3/PMP22-KK was prevalent in the perinuclear area, partially overlapping the concanavalin A staining. On the contrary, RR-Gas3/PMP22 was uniformly distributed at the cell surface. The subcellular distribution of RR-Gas3/PMP22 was indistinguishable from that of Gas3/PMP22-WT, while Gas3/PMP22-KK exhibited a subcellular distribution similar to that of Gas3/PMP22-L16P (see Figure 4).

Intracellularly Retained GAS3/PMP22 Is Unable To Regulate Both Cell Death by Apoptosis and Cell Spreading

We next analyzed whether the Gas3/PMP22-KK, which is intracellularly retained but does not present aminoacid substitutions in the transmembrane domains, was able to regulate both cell death and cell spreading.

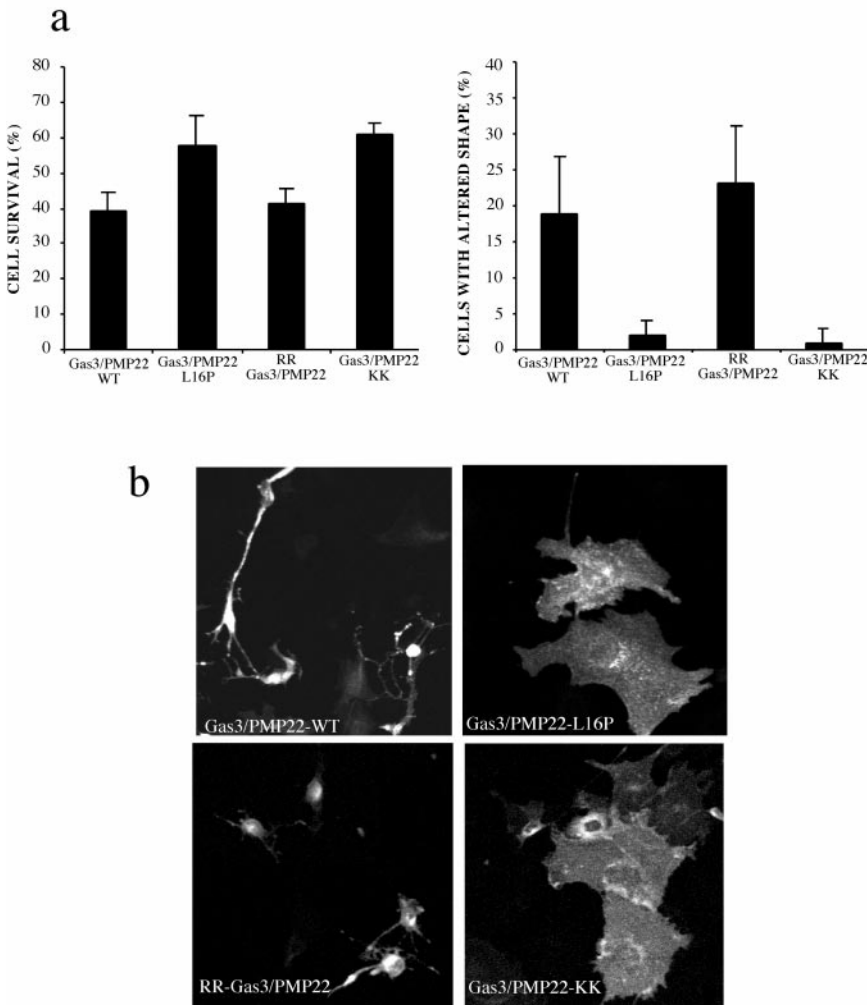Gas3/PMP22-WT, Gas3/PMP22-KK, RR-Gas3/PMP22, and the point mutant Gas3/PMP22-L16P were overexpressed by nuclear microinjection in NIH3T3 cells. All the cDNAs were cloned in the same expression vector and were microinjected at a concentration of 100 ng/μl, with hPLAP used as a reporter gene (25 ng/μl). Cells were grown for a further 18 h in 10% FCS and then were scored both for hPLAP expression and morphologic changes by immunofluorescence analysis. Cell survival and changes in cell spreading were analyzed as previously reported (Brancolini *et al.*, 1999).

Cell survival was appreciably increased in cells expressing the L16P mutants, and similar data (≈60% survival rate) were obtained in the case of intracellular retained Gas3/PMP22-KK. Gas3/PMP22-WT and RR-Gas3/PMP22 showed similar survival rates of ~40% (Figure 5a). Morphologic changes were almost undetectable when Gas3/PMP22-KK or the point mutant L16P were overexpressed. On the contrary, the overexpression of Gas3/PMP22-WT and RR-Gas3/PMP22 induced similar morphologic changes in NIH3T3 cells.

As detected after immunofluorescence analysis, representative fields of cells coexpressing hPLAP and Gas3/PMP22-WT, Gas3/PMP22-L16P, Gas3/PMP22-KK, or RR-Gas3/PMP22 are reported in Figure 5b.

Removal of the Putative Retention/Retrieval Signal from Gas3/PMP22-L16P Does not Impair Its Intracellular Sequestration

Secreted and plasma membrane proteins are assembled into their native tertiary and quaternary structure in the ER. If

Figure 5. Biological activities of the intracellularly retained Gas3/PMP22. (a) *gas3/PMP22-KK, RR-gas3/PMP22, gas3/PMP22-WT*, and *gas3/PMP22-L16P* were coexpressed with hPLAP in NIH3T3 cells. Twenty-four hours after microinjection, cells were fixed and processed by immunofluorescence to detect hPLAP. Survival and morphologic changes were scored, as described in the text. The data represent arithmetic means ± SD for four independent experiments (altered shape, p < 0.001; survival rate, p < 0.001). (b) *gas3/PMP22-KK, RR-gas3/PMP22, gas3/PMP22-WT*, and *gas3/PMP22-L16P* were coexpressed together, with hPALP as reporter gene, in NIH3T3 cells. Twenty-four hours after microinjection, cells were fixed and processed by immunofluorescence to visualize hPLAP. Bar = 5 μm.

assembly is incorrect, the protein is targeted for degradation (Zhang *et al.*, 1997). Cytoplasmic ER retention signals are present in several plasma membrane proteins where they are recognized by eukaryotic trafficking machinery. Correct assembly not only prevents protein degradation, but may also mask the ER retention/retrieval signals that allow these plasma membrane proteins to be sorted to the cell surface (Chang *et al.*, 1999; Zerangue *et al.*, 1999). The motif RKR, which is similar to ER retention/retrieval signals (Zerangue *et al.*, 1999), is present in the putative carboxyl terminal of Gas3/PMP22, and, therefore, it could mediate the retention/retrieval of the misfolded point-mutated Gas3/PMP22 (Naef and Suter, 1998). To investigate whether this tripeptide sequence was sufficient to mediate the ER retention/retrieval of point-mutated Gas3/PMP22, the tripepetide RKR was replaced with the AAA motif (Figure 6a).

Gas3/PMP22-L16P-AAA containing a VSV tag was microinjected into NIH3T3 cells, and the subcellular localization was analyzed by double-immunofluorescence analysis.

As shown in Figure 6b, Gas3/PMP22-L16P-AAA was seen most prevalently in the perinuclear area partially overlapping concanavalin A, as observed for Gas3/PMP22-L16P.

On the other hand, Gas3/PMP22-WT-AAA was uniformly distributed at the cell surface, thus indicating that the replacement of tripeptide RKR dose not interfere with the exposure at the cell surface of Gas3/PMP22. To further confirm that Gas3/PMP22-L16P-AAA was intracellularly retained, cell lysates of COS-7 cells overexpressing Gas3/PMP22-L16P-AAA were treated with Endo-H and PNGase-F. By using an antibody against the VSV, Gas3/PMP22-L16P-AAA was detected as a band migrating at around 22 kDa that was sensitive to Endo-H treatment, confirming its accumulation in an intracellular compartment before the Golgi (Figure 6c). In conclusion, Gas3/PMP22-L16-AAA shows a similar electrophoretic pattern to Gas3/PMP22-L16P.

A GAS3/PMP22 Point Mutant at the N-Glycosylation Site Is Partially Impaired in Regulating Cell Spreading but Shows Normal Apoptotic Response

The intracellularly retained Gas3/PMP22-KK was unable to trigger morphologic changes and showed reduced apoptotic
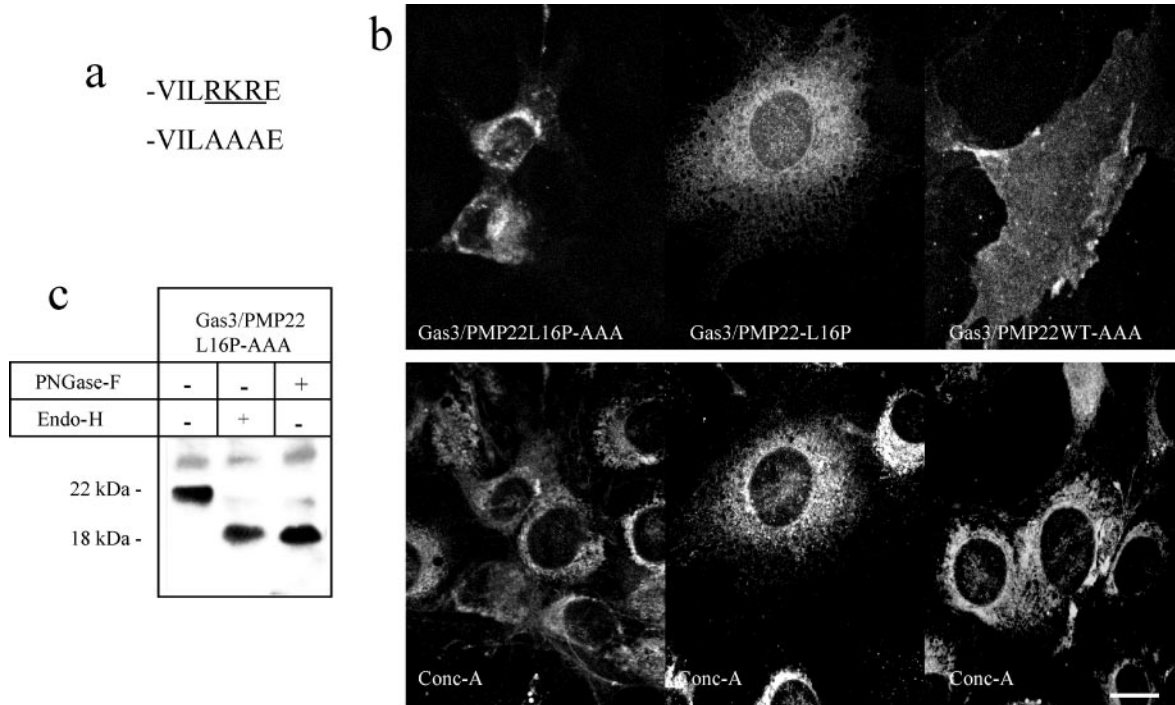
Figure 6. Subcellular localization of Gas3/PMP22-L16P-AAA. (a) Carboxyl-terminal sequence of Gas3/PMP22-WT showing the motif RKR mutated to AAA. (b) Subcellular localization of Gas3/PMP22-L16P-AAA in NIH3T3 fibroblasts. *Gas3/PMP22-L16P, Gas3/PMP22-L16P-AAA*, or *Gas3/PMP22-WT-AAA* were overexpressed in NIH3T3 cells by nuclear microinjection. Eighteen hours after microinjection, cells were fixed and double stained to visualize VSV and ER, using biotinylated concanavalin A. Bar = 25 μm. (c) Immunodetections were performed using antibodies against VSV on lysates from COS-7 cells transfected with the indicated *Gas3/PMP22-VSV* constructs. Cellular extracts were treated with or without PNGase-F and Endo-H as indicated.

response when overexpressed in NIH3T3 cells, thus indicating that exposure at the cell surface is critical for these biological activities.

Since the carbohydrate composition differs significantly between Gas3/PMP22-WT and its point-mutated derivatives that are responsible for CMT1A and DSS, we analyzed whether the carbohydrate structure plays a critical role in regulating Gas3/PMP22 biological activities. Mutagenesis of the N-glycosylation sites is widely used to assess the role of the carbohydrate chain in cell surface expression and protein activity (Levy *et al.*, 1998; Lingeman *et al.*, 1998). The asparagine residue at position 41 of Gas3/PMP22 was substituted with a glutamine residue. For clarity, we have named this mutant MG (mutant of glycosylation).

Gas3/PMP22-WT, Gas3/PMP22-L16P, and *Gas3/PMP22-MG* were transfected in COS-7 cells, and Western blot analysis was performed using an antibody against the VSV tag.

As expected, Gas3/PMP22-MG was detected as a band at 18 kDa, the intensity of which did not increase after PNGase-F treatment (Figure 7a). Gas3/PMP22-WT also was detected as a band at 18 kDa, but its intensity dramatically increased after PNGase-F treatment. The L16P point mutant was detected as a band at 22 kDa as described above.

We next analyzed the intracellular distribution of Gas3/PMP22-MG by immunofluorescence analysis. As reported in Figure 8b, Gas3/PMP22-MG shows uniform distribution at

the plasma membrane and is indistinguishable from the subcellular distribution of Gas3/PMP22-WT. This indicates that the N-glycosylation does not interfere with the intracellular trafficking of Gas3/PMP22.

To understand whether N-glycosylation of Gas3/PMP22 is required for regulating cell spreading and apoptosis, Gas3/PMP22-MG was overexpressed by nuclear microinjection into NIH3T3 cells. *hPLAP* was used as reporter gene, and a time course analysis was performed (Figure 8).

Gas3/PMP22-MG reduced cell survival in a manner similar to Gas3/PMP22, while the intracellularly retained Gas3/PMP22-KK did not. A 30% survival rate 24 h after microinjection for both Gas3/PMP22-WT and Gas3/PMP22-MG was observed, while the survival rate for Gas3/PMP22-KK was 60%. These values did not change at different time points after microinjection.

A different scenario was observed when changes in cell spreading were analyzed 18 h after microinjection, Gas3/PMP22-WT induced changes in cell spreading in ~30% of the injected cells, reaching ~50% of the injected cells 30 h after microinjection.

Gas3/PMP22-MG was partially impaired in regulating cell shape changes; in fact, 18 h after microinjection ~10% of cells showed changes in cell spreading, peaking at 30% 30 h after microinjection. Intracellularly retained Gas3/PMP22-KK was unable to regulate changes in cell spreading.
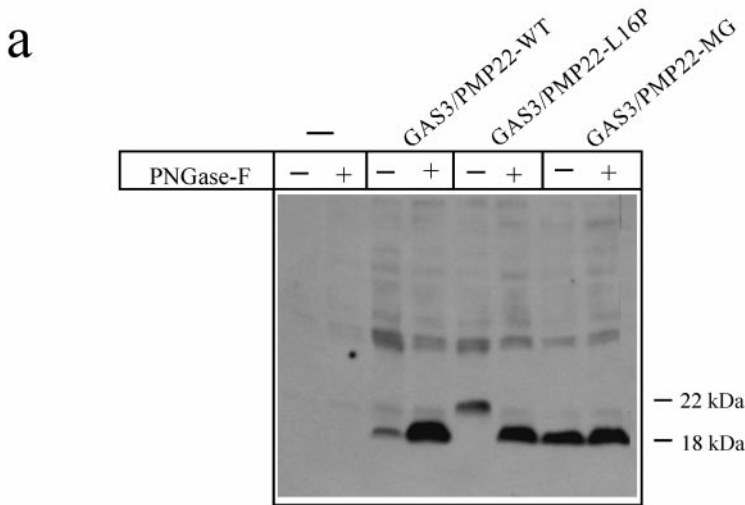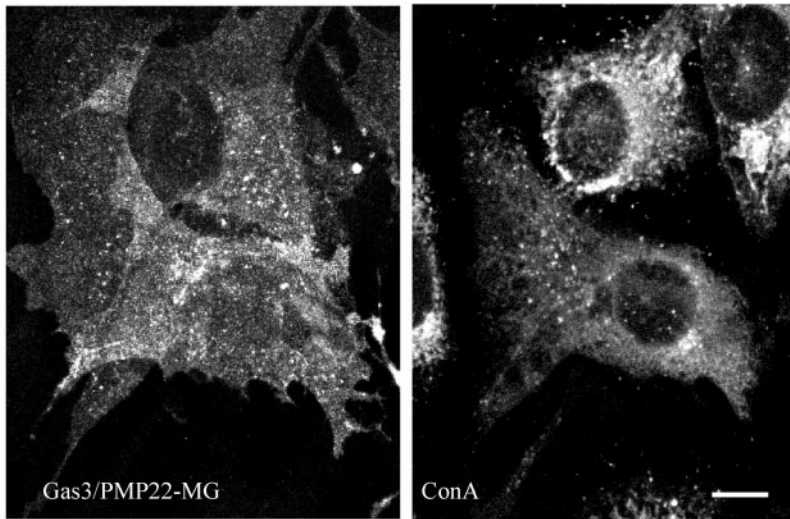
Figure 7. Expression and subcellular localization of Gas3/PMP22 mutated at the N-glycosylation site. (a) Immunodetections were performed using antibodies against VSV on lysates from COS-7 cells transfected with the indicated *Gas3/PMP22-VSV* constructs. Cellular extracts were treated with or without PNGase-F as indicated. (b) Double-immunofluorescence analysis of NIH3T3 expressing Gas3/PMP22-MG-VSV and double stained for VSV and concanavalin A. Fifteen hours after microinjection, cells were fixed and processed by immunofluorescence. Bar 15=μm.

DISCUSSION

Differences in the Intracellular Localization of WT and Point-Mutated Gas3/PMP22

We generated different epitope tags for Gas3/PMP22 to explore the intracellular localization of the WT form with respect to its point-mutated derivatives that are responsible for CMT1A and DSS. The epitope tags were inserted at the carboxyl terminus of the protein, where they do not trigger harmful effects on Gas3/PMP22 (Naef *et al.*, 1997; D'Urso *et al.*, 1998). In fact, when overexpressed in different cells, epitope-tagged Gas3/PMP22 was indistinguishable from the untagged Gas3/PMP22 in terms of its ability to induce cell death and changes in cell spreading (Brancolini *et al.* 1999; our unpublished results).

In Western blot analysis, both the VSV and the FLAG epitope tags fused to Gas3/PMP22-WT allowed the detection of an 18-kDa form that lacks the N-linked sugar chain (Manfioletti *et al.*, 1990; Pareek *et al.*, 1993). When a paired VSV epitope was used, the mature 22-kDa form of Gas3/PMP22 was detected. It should be emphasized that by using the paired VSV epitope the majority of Gas3/PMP22 was detected as an unresolved smear ranging from ~30 kDa to 55 kDa. The smear was sensitive to PNGase-F treatments but not to Endo-H treatments (our unpublished results). Taking into account that the detection of Gas3/PMP22 dimers in lysates from the sciatic nerve was sensitive to PNGase-F treatment (Tobler *et al.*, 1999), we suggest that the observed smear might be dependent both on dimer formation and on heterogeneity in the oligosaccharide chains as a result of a transition through the Golgi apparatus (Kaushal *et al.* 1994).
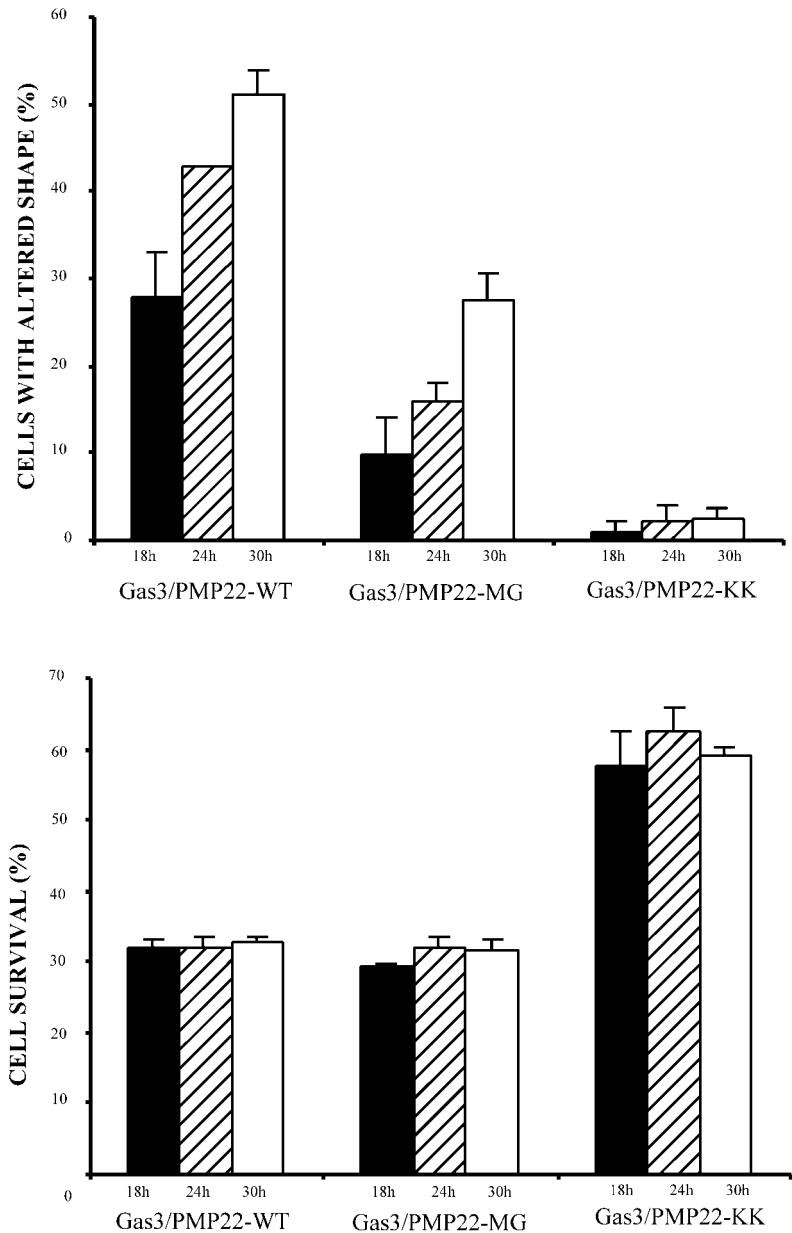
Figure 8. Biological activities of Gas3/PMP22 mutated at the N-glycosylation site. *gas3/PMP22-MG*, *gas3/PMP22-WT*, and *gas3/PMP22-KK* were coexpressed with hPLAP in NIH3T3 cells. At different time points after microinjection, cells were fixed and processed by immunofluorescence to detect hPLAP. Survival and morphologic changes were scored as described in the text. The data represent the arithmetic means ± SD of four independent experiments (altered shape, $p < 0.001$; survival rate, $p < 0.001$)

Based on this evidence, we cannot clearly state whether the sugar chain or the dimer formation in Gas3/PMP22 influence the detection of the eiptope tags when inserted at its carboxyl terminus.

The Gas3/PMP22 point-mutated versions were seen by Western blot analysis as 22-kDa forms that shifted to 18-kDa forms after PNGase-F treatment. This result clearly indicates a profound difference in terms of the N-glycosylation pattern between the Gas3/PMP22-WT and the point mutants that were analyzed. The different N-glycosylation reflects the different subcellular localization of the Gas3/PMP22-WT with respect to the point-mutated form (Tobler *et al.*, 1999). Confocal analysis, biotinylation of plasma membrane proteins, and different sensitivity to Endo-H glycosidase indicate that Gas3/

PMP22-WT is exposed at the cell surface, while the point mutants L16P, S79C, and G150D are retained intracellularly before the Golgi. These observations corroborate previous reports showing that different point-mutated forms of Gas3/PMP22 accumulated intracellularly (Naef *et al.*, 1997; D'Urso *et al.*, 1998; Naef and Suter 1999; Tobler *et al.*, 1999).

The Tripeptide RKR Present in the Carboxyl Terminal of Gas3/PMP22 Is Not Sufficient for the Intracellular Sequestration of its Point-Mutated Form

In the studies mentioned above, Gas3/PMP22 point mutations located in the transmembrane domains have been

used; therefore, the overall folding of the protein may well have been altered. Intracellular retention of the misfolded protein then would be mediated by quality control in the ER.

A wide range of debilitating human diseases is associated with protein-misfolding events (Dobson, 1999). Secreted and plasma membrane proteins are assembled into their native tertiary and quaternary structure in the ER. If assembly is incorrect, the protein is detected and targeted for degradation (Zhang *et al.*, 1997). In the case of CFTR mutations, it seems possible that the native conformation is the crucial parameter determining whether or not it is permitted to depart from the ER. Recently it has been proposed that export-incompetent mutants of CFTR display multiple arginine-framed tripeptide sequences, which are important for the intracellular retention/retrieval that is mediated by ER quality control (Chang *et al.*, 1999). In the case of the ATP-sensitive K+ channel, it has been established that quality control in the assembly of multimeric channels depends on a three-amino acid trafficking motif, RKR, that is present in the cytoplasmic loops of the proteins (Zerangue *et al.*, 1999).

Interestingly, the motif RKR is present in the cytoplasmic carboxyl terminal of Gas3/PMP22 (Naef and Suter, 1998). However, the replacement of the RKR sequence with AAA in the point-mutated L16P did not enable its surface expression, suggesting that additional mechanisms are responsible for its intracellular retention.

Cell Surface Expression of Gas3/PMP22 Is Required for its Signaling Activities

If Gas3/PMP22 misfolding was responsible for its intracellular retention, we cannot distinguish whether the failure of the point-mutated forms of Gas3/PMP22 to regulate cell death and changes in cell spreading was caused by an altered folding or by a failure to reach the cell surface. To answer this question, we have created a Gas3/PMP22 that is without amino acid substitutions in the transmembrane domains but that is defective in its ability to reach the cell surface due to a carboxyl-terminal retention/retrieval signal KK (Teasdale and Jackson, 1996). Similar to the Gas3/PMP22 point-mutated forms responsible for CMT1A and the DSS, Gas3/PMP22-KK was unable to regulate cell death and cell spreading. Its presence at the cell surface is, therefore, the prerequisite for its signaling activities. This result implies that the effects on cell shape and death are not due to a toxic effect that is dependent on the overexpression of the protein but, probably, is dependent on the formation of a signaling complex at the plasma membrane, the activity of which might be strictly related to the diseases.

How can Gas3/PMP22 modulate cell death and cell spreading when exposed at the cell surface? It is possible that Gas3/PMP22 needs to form a signaling complex that interacts with different partners and that this complex only can be assembled at the plasma membrane.

A partner for Gas3/PMP22 recently has been identified as the P0 protein (D'Urso *et al.*, 1999). Since we have already observed that P0 was unable to regulate both apoptosis and changes in cell spreading, it will be interesting to test whether P0 can modulate the signaling function of Gas3/PMP22. However, the recent generation of mice deficient both in P0 and PMP22 suggests different roles for these proteins in myelin formation and maintenance (Carenini *et al.*, 1999).

The diseases caused by the point-mutated versions of Gas3/PMP22 usually are more severe than the ones caused by Gas3/PMP22 duplication, even though there are differences depending on the type and the location of the amino acid change (Suter and Snipes, 1995; Naef *et al.*, 1997; D'Urso *et al.*, 1998; Kovach *et al.*, 1999; Nelis *et al.*, 1999; Tobler *et al.*, 1999).

This observation indicates that the point-mutated forms of Gas3/PMP22 act by a gain of function. Two possible pathologic mechanisms for peripheral neuropathies caused by mutations of Gas3/PMP22 have been proposed: (1) overloading and subsequent alteration of the endoplasmic reticulum–Golgi compartments as a consequence of the failure of the point-mutated forms to reach the cell surface (D'Urso *et al.*, 1998; Hanemann and Muller, 1998); and (2) intracellular retention of Gas3/PMP22-WT as a direct consequence of a heterodimer formation with the point-mutated forms (Naef *et al.*, 1997; Tobler *et al.*, 1999).

Our observation that impairment of the exposure of Gas3/PMP22-WT at the cell surface is sufficient to switch off its biological activities favors the hypothesis of an effect of the point-mutated Gas3/PMP22 on Gas3/PMP22-WT intracellular trafficking.

N-Glycosylation of Gas3/PMP22 Is Required for a Full Effect on Cell Spreading

In Schwann cells, Gas3/PMP22 contains a carbohydrate determinant reacting with the HNK1 monoclonal antibody, which is generally expressed on adhesion molecules (Hammer *et al.*, 1993; Pareek *et al.*, 1993; Snipes *et al.*, 1993). Since a major difference between Gas3/PMP22-WT and the point-mutated derivatives is the carbohydrate moiety, we have analyzed whether N-glycosylation can influence the signaling function of Gas3/PMP-WT. A Gas3/PMP22 with a substitution Asn/Gln at the N-glycosylation site was exposed normally at the plasma membrane. This mutant was indistinguishable from the WT in its ability to induce cell death but was partially impaired in triggering cell-spreading changes.

It has been demonstrated that N-glycosylation of Gas3/PMP22 is not required for interaction with P0, while the identification of a putative Gas3/PMP22 dimer is sensitive to PNGase treatment (D'Urso *et al.*, 1999; Tobler *et al.*, 1999). In this context, it could be possible that the reduced ability of Gas3/PMP22 lacking the N-glycosylation site to regulate cell spreading might be dependent on a reduced ability to form stable homodimers at the plasma membrane. Alternatively, since we have already demonstrated that Gas3/PMP22 can independently regulate cell death and spreading, the carbohydrate structure might be directly involved in establishing a stable relationship with a plasma membrane component involved in regulating cell spreading. In the future, we plan to dissect the molecular complex containing Gas3/PMP22 at the plasma membrane.

ACKNOWLEDGMENTS

REFERENCES

Agostoni, E., Gobessi, S., Brancolini, C., and Schneider, C. (1999). Identification and characterization of a new member of the gas3/PMP22 gene family in *C. elegans*. Gene *234*, 267–274.

Adlkofer, K., Martini, R., Aguzzi, A., Zielasek, J., Toyka, K.V., and Suter, U. (1995). Hypermyelination and demyelinating peripheral neuropathy in PMP22-deficient mice. Nat. Genet. *11*, 274–280.

Baechner, D., Liehr, T., Hameister, H., Altenberger, H., Grehl, H., Suter, U., and Rautenstrauss, B. (1995). Widespread expression of the peripheral myelin protein-22 gene (pmp22) in neural and non-neural tissue during murine development. J. Neurosci. Res. *42*, 733–741.

Baudet, C., Perret, E., Delpech, B., Kaghad, M., Brachet, P., Wion, D., and Caput, D. (1998). Differentially expressed genes in C6.9 glioma cells during vitamin D-induced cell death program. Cell Death Differ. *5*, 116–125.

Brancolini, C., Marzinotto, S., and Schneider, C. (1997). Susceptibility to p53 dependent apoptosis correlates with increased levels of Gas2 and Gas3 proteins. Cell Death Diff. *4*, 247–253.

Brancolini, C., Marzinotto, S., Edomi, P., Agostoni, E., Fiorentini, C., Muller, H.W., and Schneider, C. (1999). Rho-dependent regulation of cell spreading by the tetraspan membrane protein Gas3/PMP22. Mol. Biol. Cell *10*, 2441–2459.

Carenini, S., Neuberg, D., Schachner, M., Suter, U., and Martini, R. (1999). Localization and functional roles of PMP22 in peripheral nerves of P0-deficient mice. Glia *28*, 256–264.

Chang, X.B., Cui, L., Hou, Y.X., Jensen, T.J., Aleksandrov, A.A., Mengos, A., and Riordan, J.R. (1999). Removal of multiple arginine-framed trafficking signals overcomes misprocessing of delta F508 CFTR present in most patients with cystic fibrosis. Mol. Cell. *4*, 137–142.

Dobson, C.M. (1999). Protein misfolding evolution and disease. Trends Biochem. Sci. *24*, 329–332.

D'Urso, D., Prior, R., Greiner-Petter, R., Gabreels-Festen, A.A., and Muller, H.W. (1998). Overloaded endoplasmic reticulum-Golgi compartments, a possible pathomechanism of peripheral neuropathies caused by mutations of the peripheral myelin protein PMP22. J. Neurosci. *18*, 731–740.

D'Urso, D., Ehrhardt, P., and Muller, H.W. (1999). Peripheral myelin protein 22 and protein zero: a novel association in peripheral nervous system myelin. J. Neurosci. *19*, 3396–3403.

Edomi, P., Martinotti, A., Colombo, M.P., and Schneider, C. (1993). Sequence of human *gas3/PMP22* full-length cDNA. Gene *126*, 289–290.

Fabbretti, E., Edomi, P., Brancolini, C., and Schneider, C. (1995). Apoptotic phenotype induced by overexpression of the wilde type gas3/PMP22: its relation to the demyelinating peripheral neuropathy CMT1A. Genes Dev. *9*, 1846–1856.

Hammer, J.A., O'Shannessy, D.J., De Leon, M., Gould, R., Zand, D., Daune, G., and Quarles, R.H. (1993). Immunoreactivity of PMP-22, P0, and other 19 to 28 kDa glycoproteins in peripheral nerve myelin of mammals and fish with HNK1 and related antibodies. J. Neurosci. Res. *35*, 546–558.

Hanemann, C.O., and Muller, H.W. (1998). Pathogenesis of Charcot-Marie-Tooth 1A (CMT1A) neuropathy. Trends Neurosci. *21*, 282–286.

Huxley, C., Passage, E., Manson, A., Putzu, G., Figarella-Branger, D., Pellissier, J.F., and Fontes, M. (1996). Construction of a mouse model of Charcot-Marie-Tooth disease type 1A by pronuclear injection of human YAC DNA. Hum. Mol. Genet. *5*, 563–569.

Jackson, M.R., Nilsson, T., and Peterson, P.A. (1990). Identification of a consensus motif for retention of transmembrane proteins in the endoplasmic reticulum. EMBO J. *9*, 3153–3162.

Ionasescu, V.V., Searby, C., and Greenberg, S.A. (1996). Dejerine-Sottas disease with sensorineural hearing loss, nystagmus, and peripheral facial nerve weakness: de novo dominant point mutation of the PMP22 gene. J. Med. Genet. *33*, 1048–1049.

Kaushal, S., Ridge, K.D., and Khorana, H.G. (1994). Structure and function in rhodopsin: The role of asparagine-linked glycosylation. Proc. Natl. Acad. Sci. USA *91*, 4024–4028.

Kornfeld, R., and Kornfeld, S. (1985). Assembly of asparagine-linked oligosaccharides. Annu. Rev. Biochem. *54*, 631–664.

Kovach, M.J., Lin, J.P., Boyadjiev, S., Campbell, K., Mazzeo, L., Herman, K., Rimer, L.A., Frank, W., Llewellyn, B., Wang Jabs, E., Gelber, D., and Kimonis, V.E. (1999). A unique point mutation in the PMP22 gene is associated with Charcot-Marie-Tooth disease and deafness. Am. J. Hum. Genet. *64*, 1580–1593.

Levy, O., De la Vieja, A., Ginter, C.S., Riedel, C., Dai, G., and Carrasco, N. (1998). N-linked glycosylation of the thyroid Na+/I-symporter (NIS): implications for its secondary structure model. J. Biol. Chem. *273*, 22657–22663.

Lingeman, R.G., Joy, D.S., Sherman, M.A., and Kane, S.E. (1998). Effect of carbohydrate position on lysosomal transport of procathepsin L. Mol. Biol. Cell. *9*, 1135–1147.

Lupski, J.R., Montes de Oca Luna, R., Slaugenhaupt, S., Pentao, L., Guzzetta, V., Trask, B.J., Saucedo-Cordenas, O., Barker, D.F., Killian, J.M., Garcia, C.A., Chakravarti, A., and Patel, I.P. (1991). DNA duplication associated with Charcot-Marie-Tooth disease type 1A. Cell *66*, 219–232.

Magyar, J.P., Martini, R., Ruelicke, T., Aguzzi, A., Adlkofer, K., Dembic, Z., Zielasek, J., Toyka, K.V., and Suter, U. (1996). Impaired differentiation of Schwann cells in transgenic mice with increased PMP22 gene dosage. J. Neurosci. *16*, 5351–53060.

Manfioletti, G., Ruaro, M.E., Del Sal, G., Philipson, L., and Schneider, C. (1990). A growth arrest -specific (gas) gene codes for a membrane protein. Mol. Cell. Biol. *10*, 2924–2930.

Matsunami, N., Smith, B., Ballard, L., Lensch, M.W., Robertson, M., Albertsen, H., Hanemann, C.O., Müller, H.W., Bird, T.D., White, R., and Chance, P.F. (1992). Peripheral myelin protein-22 gene maps in the duplication in chromosome 17p11.2 associated with Charcot-Marie-Tooth type 1A. Nat. Genet. *1*, 176–179.

Naef, R., Adlkofer, K., Lescher, B., and Suter, U. (1997). Aberrant protein trafficking in Trembler suggests a disease mechanism for hereditary human peripheral neuropathies. Mol. Cell. Neurosci. *1*, 13–25.

Naef, R., and Suter, U. (1998). Many facets of the peripheral myelin protein PMP22 in myelination and disease. Microsc. Res. Tech. *41*, 359–371.

Naef, R., and Suter, U. (1999). Impaired intracellular trafficking is a common disease mechanism of PMP22 point mutations in peripheral neuropathies. Neurobiol. Dis. *6*, 1–14.

Nelis, E., Haites, N., and Van Broeckhoven, C. (1999). Mutations in the peripheral myelin genes and associated genes in inherited peripheral neuropathies. Hum. Mutat. *13*, 11–28.

Pareek, S., Suter, U., Snipes, G.J., Welcher, A.A., Shooter, E.M., and Murphy, R.A. (1993). Detection and processing of peripheral myelin protein PMP22 in cultured Schwann cells. J. Biol. Chem. *268*, 10372–10379.

Patel, P.I., Roa, B.B., Welcher, A.A., Schoener-Scott, R., Trask, B.J., Pentao, L., Snipes, G.J., Garcia, C.A., Francke, U., Shooter, E.M., Lupski, J.R., and Suter, U. (1992). The gene for the peripheral myelin

protein PMP-22 is a candidate for Charcot-Marie-Tooth disease type 1A. Nat. Genet. *1*, 159–165.

Patel, I.P., and Lupski, J.R. (1994). Charcot-Marie-Tooth disease: a new paradigm for the mechanism of inherited disease. Trends Genet. *10*, 128–133.

Roa, B.B., Dyck, P.J., Marks, H.G., Chance, P.F., and Lupski, J.R. (1993a). Dejerine-Sottas syndrome associated with point mutation in the peripheral myelin protein 22 (PMP22) gene. Nat. Genet. *5*, 269–273.

Roa, B.B., Garcia, C.A., Suter, U., Kulpa, D.A., Wise, C.A., Müller, J., Welcher, A.A., Snipes, G.J., Shooter, E.M., and Patel, P. (1993b). Charcot-Marie-Tooth disease type 1A. Association with a spontaneous point mutation in the PMP22 gene. N. Engl. J. Med. *329*, 96–101.

Schutze, M-P., Peterson, P.A., and Jackson, M.R. (1994). An N-terminal. double-arginine motif mantains type II membrane proteins in the endoplasmic reticulum. EMBO J., *13*, 1696–1705.

Sereda, M., Griffiths, I., Puhlhofer, A., Stewart, H., Rossner, M.J., Zimmermann, F., Magyar, J.P., Schneider, A., Hund, E., Meinck, H.-M., Suter, U., and Nave, K.-A. (1996). A transgenic rat model of Charcot-Marie-Tooth disease. Neuron *16*, 1049–1060.

Snipes, G.J., Suter, U., Welcher, A.A., and Shooter, E.M. (1992). Characterization of a novel peripheral nervous system myelin protein (PMP22/SR13). J. Cell. Biol. *117*, 225–238.

Snipes, G.J., Suter, U., and Shooter, E.M. (1993). Human peripheral myelin protein-22 carries the L2/HNK-1 carbohydrate adhesion epitope. J. Neurochem. *61*, 1961–1964.

Spreyer, P., Kuhn, G., Hanemann, C.O., Gillen, C., Schaal, H., Kuhn, R., Lemke, G., and Müller, H.W. (1991). Axon-regulated expression of a Schwann cell transcript that is homologous to a "growth arrest-specific" gene. EMBO J. *10*, 3661–3668.

Suter, U., and Snipes, J.C. (1995). Biology and genetics of hereditary motor and sensory neuropathies. Annu. Rev. Neurosci. *18*, 45–75.

Teasdale, R.D., and Jackson, M.R. (1996). Signal-mediated. sorting of membrane proteins between the endoplasmic reticulum and the Golgi apparatus. Annu. Rev. Cell Dev. Biol *12*, 27–54.

Tobler, A.R., Notterpek, L., Naef, R., Taylor, V., Suter, U., and Shooter, E.M. (1999). Transport of Trembler-J mutant peripheral myelin protein 22 is blocked in the intermediate compartment and affects the transport of the wild-type protein by direct interaction. J. Neurosci. *19*, 2027–2036.

Timmerman, V., Nelis, E., Van Hul, W., Nieuwenhuijsen, B.W., Chen, K.L., Wang, S., Ben Othman, K., Cullen, B., Leach, R.J., Hanemann, C.O., De Jonghe, P., Raeymaekers, P., van Ommen, G.-J.P., Martin, J.J., Müller, H.W., Vance, J.M., Fischbeck, K.H., and Van Broeckhoven, C. (1992). The peripheral myelin protein gene PMP22 is contained within the Charcot-Marie-Tooth disease type 1A duplication. Nat. Genet. *1*, 171–175.

Valentijn, L.J., Baas, F, Wolterman, R.A., Hoogendijk, J.E., van den Bosch, N.H.A., Zorn, I., Gabreels-Festen, W, M., de Visser, M., and Bolhuis, P.A. (1992a). Identical point mutations of PMP-22 in Trembler-J mouse and Charcot-Marie-Tooth disease type 1A. Nat. Genet. *2*, 288–291.

Valentijn, L.J., Bolhuis, P.A., Zorn, I., Hoogendijk, J.E., van den Bosch, N., Hensels, G.W., Stanton, V.P., Jr., Housman, D.E., Fishbeck, K.H., Ross, D.A., Nicholson, G.A., Meershoek, E.J., Dauwerse, H.G., van Ommen, G.-J.B., and Baas, F. (1992b). The peripheral myelin gene PMP-22/GAS-3 is duplicated in Charcot-Marie-Tooth disease type 1A. Nat. Genet. *1*, 166–170.

Welcher, A.A., Suter, U., De Leon, M., Snipes, G.J., and Shooter, E.M. (1991). A myelin protein is encoded by the homologue of a growth arrest-specific gene. Proc. Natl. Acad. Sci. USA *88*, 7195–7199.

Wulf, P., Bernhardt, R.R., and Suter, U. (1999). Characterization of peripheral myelin protein 22 in zebrafish (zPMP22) suggests an early role in the development of the peripheral nervous system. J. Neurosci. Res. *57*, 467–478.

Zerangue, N., Schwappach, B., Jan, Y.N., and Jan, L.Y. (1999). A new ER trafficking signal regulates the subunit stoichiometry of plasma membrane K(ATP) channels. Neuron *22*, 537–548.

Zhang, J.-X., Braakman, I., Matlack, K.E.S., and Helenius, A. (1997). Quality control in the secretory pathway: the role of calreticulin, calnexin and BiP in the retention of glycoproteins with C-terminal truncations. Mol. Biol. Cell *8*, 1943–1954.

Zoidl, G., D'Urso, D., Blass-Kampamann, S., Schmalenbach, C., Kuhn, R., and Muller, H.W. (1997). Influence of elevated expression of rat wild-type PMP22 and its mutant PMP22Trembler on cell growth of NIH3T3 fibroblasts. Cell Tissue Res. *287*, 459–470.